HHS Public Access

Author manuscript

Clin Cancer Res. Author manuscript; available in PMC 2020 June 15.

Published in final edited form as:

Clin Cancer Res. 2019 June 15; 25(12): 3561–3571. doi:10.1158/1078-0432.CCR-18-3267.

CD47-targeted Near-Infrared Photoimmunotherapy for Human Bladder Cancer

Bernhard Kiss[1,2], **Nynke S. van den Berg**[3], **Robert Ertsey**[3], **Kelly McKenna**[4], **Kathleen E. Mach**[1,5], **Chiyuan Amy Zhang**[1], **Jens-Peter Volkmer**[4], **Irving L. Weissman**[2], **Eben L. Rosenthal**[3], **Joseph C. Liao**[1,5]

[1]Department of Urology, Stanford University School of Medicine, Stanford, California

[2]Institute for Stem Cell Biology and Regenerative Medicine, Stanford University, Stanford, California

[3]Department of Otolaryngology–Head and Neck Surgery, Stanford University School of Medicine, Stanford, California.

[4]Forty Seven Inc., Menlo Park, California

[5]Veterans Affairs Palo Alto Health Care System, Palo Alto, California

Abstract

Purpose: Near-infrared photoimmunotherapy (NIR-PIT) is a localized molecular cancer therapy combining a photosensitizer-conjugated monoclonal antibody and light energy. CD47 is an innate immune checkpoint widely expressed on bladder cancer cells but absent from luminal normal urothelium. Targeting CD47 for NIR-PIT has the potential to selectively induce cancer cell death and minimize damage to normal urothelium.

Experimental design: The cytotoxic effect of NIR-PIT with anti-CD47-IR700 was investigated in human bladder cancer cell lines and primary human bladder cancer cells derived from fresh surgical samples. Phagocytosis assays were performed to evaluate macrophage activity after NIR-PIT. Anti-CD47-IR700 was administered to murine xenograft tumor models of human bladder cancer for *in vivo* molecular imaging and NIR-PIT.

Results: Cytotoxicity in cell lines and primary bladder cancer cells significantly increased in a light-dose dependent manner with CD47-targeted NIR-PIT. Phagocytosis of cancer cells significantly increased with NIR-PIT compared to antibody alone ($p=0.0002$). *In vivo* fluorescence intensity of anti-CD47-IR700 in tumors reached a peak 24-hour post injection and was detectable for at least 14 days. After a single round of CD47-targeted NIR-PIT, treated animals showed significantly slower tumor growth compared to controls ($p<0.0001$). Repeated CD47-targeted

Corresponding Author: Joseph C. Liao, M.D., Department of Urology, 300 Pasteur Dr., Room S-287, Stanford, CA 94305-5118, USA; Phone: 650-858-3916; Fax: 650-849-0319; jliao@stanford.edu.

Conflict of interest statement:
Irving Weissman is co-founder, a member of the Board of Directors, a consultant, and owns equity in Forty Seven Inc. Jens-Peter Volkmer is co-founder, an employee and owns equity in Forty Seven Inc. Kelly McKenna owns equity in Forty Seven Inc. The remainder of authors declare no potential conflicts of interest.

NIR-PIT treatment further slowed tumor growth (p=0.0104) and improved survival compared to controls.

Conclusion: CD47-targeted NIR-PIT increased direct cancer cell death and phagocytosis resulting in inhibited tumor growth and improved survival in a murine xenograft model of human bladder cancer.

Keywords

CD47 antigen; phototherapy; bladder cancer; molecular imaging; theranostics

Introduction

The majority of patients with bladder cancer, the sixth most common cancer, present with early stage (Ta, T1, TIS) disease and are treated by endoscopic resection and intravesical therapy (1). With a one-year recurrence rate of up to 61%, bladder cancer has one of the highest recurrence rates among all solid cancers (2). High risk non-muscle-invasive bladder cancer (NMIBC) has a 5-year progression rate to muscle invasive bladder cancer (MIBC) of 20% (3). For MIBC, neoadjuvant chemotherapy combined with radical cystectomy is the first-line treatment, with cancer-specific survival rate of 35% after 4 years (4). Therefore, optimizing detection and resection of early stage bladder cancer is critical.

White light cystoscopy (WLC) and WLC-assisted transurethral resection of bladder tumor (TURBT) are the standard for detection, resection, and surveillance of bladder cancer. WLC and TURBT have well-recognized shortcomings including missed tumors, incomplete resection, and understaging (5). Increasingly, adjunctive optical imaging technologies are utilized to augment WLC (6). Photodynamic diagnosis (PDD), based on intravesical administration of the photosensitizer hexaminolevulinate (HAL) coupled with blue light cystoscopy, improves bladder cancer detection and is increasingly clinically utilized (7). Photodynamic therapy (PDT) combines cellular uptake of a photosensitizer and light exposure to induce cell death. The feasibility and safety of PDT using the photosensitizers HAL or Radiochlorine® have been tested in small clinical trials (8, 9). Due to lack of specificity of the photosensitizer, long irradiation times, and significant local side effects, PDT has not been widely adopted clinically for bladder cancer (8-12).

Near-infrared photoimmunotherapy (NIR-PIT) is a molecular targeted therapy that combines target specificity of a monoclonal antibody conjugated with IRDye700, a hydrophilic phthalocyanine dye that is activated by NIR light (11, 13). The mechanism of action is based on generation of reactive oxygen and singlet oxygen species, resulting in cell rupture and necrosis (11, 13). The longer excitation wavelength used for NIR-PIT compared to conventional PDT results in deeper tissue penetration (12-14), while high target specificity conferred by the monoclonal antibody reduces nonspecific local toxicity. NIR-PIT has been successfully demonstrated in cell lines, xenograft tumor mouse models, and is being tested in an ongoing clinical trial for head and neck squamous cell carcinoma (ClinicalTrials.gov NCT02422979) (11, 13, 15). For bladder cancer, epidermal growth factor receptor (EGFR)-targeted NIR-PIT has been successfully demonstrated *in vitro* and in xenograft models *in vivo* (11). However, EGFR-targeted NIR-PIT is unlikely to be widely applicable, as EGFR

amplification is only found in approximately 11% of bladder tumors (11, 16). Targeting a more abundant surface antigen can potentially lead to a broader applicability of NIR-PIT in bladder cancer.

CD47 is a cell surface protein that mediates neutrophil migration and T-cell co-stimulation (17-19). Blocking the interaction of CD47 with its native ligand SIRPα promotes phagocytosis of the CD47-expressing cells and prevents metastasis of human solid tumors in mouse xenograft models (18). In characterization of bladder tumor initiating cells, CD47 was found expressed in all human bladder tumors examined with the highest level of expression in the CD44+ cells (20). Further, CD47 is highly expressed in both NMIBC and MIBC, but absent on the terminally differentiated luminal umbrella cells of normal human bladder urothelium (21). CD47 has been demonstrated to be a promising optical molecular imaging target for bladder cancer (21). The safety and therapeutic efficacy of anti-CD47 is being investigated in several clinical trials for a variety of hematopoietic and solid cancers (22) (ClinicalTrials.gov NCT02216409).

In this study, we investigated anti-CD47-IR700 as a molecular photosensitizer for NIR-PIT of bladder cancer. We assessed CD47-targeted NIR-PIT in established human bladder cancer lines for assay development, then tested the *in vitro* protocol on primary human bladder cancer cells derived from fresh surgical samples. Finally, we demonstrate that CD47-targeted NIR-PIT effectively inhibits growth of human bladder cancer tumors *in vivo* in a xenograft mouse model.

Materials and methods

Synthesis of anti-CD47-IR700

Mouse anti-human CD47 monoclonal antibody (B6H12) was conjugated with IRDye700DX per manufacturer's protocol (Li-Cor Biosciences). Briefly, anti-CD47 (1 mg/ml) was incubated with 8 μg IRDye700DX NHS ester for 2 hours at room temperature. Free dye was removed by purification on a Zeba™ desalting column and the antibody concentration was determined with Coomassie Plus (Thermo Fisher Scientific) by measuring the absorption at 593nm with UV-Vis spectrophotometer (Thermo Fisher Scientific). The labeled antibody was characterized by SDS-PAGE and electrospray ionization mass spectrometry (ESI-MS) on a Agilent 1260 HPLC and Bruker MicroTOF-Q II as previously described (23). Spectra were collected in full scan MS mode with a mass range of 900-4000 Da and collision RF setting of 1200 Vpp.

Human bladder cancer cell lines

UMUC-3 and HT-1376 were obtained from the American Type Culture Collection (ATCC). 639V was previously obtained from the German Resource Centre for Biological Material (DSMZ) and transfected with a GFP-luciferase encoding lentivirus (24). All three cell lines were derived from high grade human bladder tumors and all have mutation in TP53. 639V and UMUC-3 were obtained from males and HT-1376 is from a female. According to the UBC 40 urothelial bladder cancer cell line index (25), 639V and UMUC 3 have a high genome instability and HT-1376 has low genome instability. Additional oncogene mutations

include KRAS in UMUC-3, RB1 in HT1376 and PIK3CA in 639V cells. Cell lines were cultured in a humidified incubator at 37°C with 5% CO_2. 639V and HT-1376 were cultured in DMEM (Gibco) supplemented with 10% fetal bovine serum and 1% penicillin/ streptomycin (Life Technologies). UMUC3 was grown in MEM including Earl's salts supplemented with 1% non-essential amino acids, 1% pyruvate, 2% bicarbonate, 10% fetal bovine serum and 1% penicillin/ streptomycin.

In vitro NIR-PIT of bladder cancer cell lines

Bladder cancer cells of all 3 cell lines were removed from plates using 1x TrypLE (Gibco), washed with serum-free PBS, after which 1.5×10^6 cells were incubated with PBS, PBS containing 8 μg/mL anti-CD47 (only UMUC3 and 639V) or PBS containing 8 μg/mL anti-CD47-IR700 for 1 hour in the dark on ice. Cells were then seeded into 96-well low adhesion plates (50,000 cells per well) and irradiated with a red (690-710 nm) light-emitting diode (Thorlabs, M680L4). The light source was positioned 0.2-0.3cm over the cells and produced a power density of 50 mW/cm^2 as determine by an optical power meter (Thorlabs, PM 100) (13). Light energy levels used for cells incubated with anti-CD47-IR700 were 0, 1, 2, 5, 10, 20 or 40 Joules/cm^2 (J/cm^2) with a maxium exposure time of 9.3 minutes for 40 J/cm^2. Cells incubated with unlabeled anti-CD47 received 40 J/cm^2. Thirty minutes after the various experimental conditions propidium iodide (Thermo Fisher Scientific) was added to the cells to achieve final concentration of 1 μg/mL and incubated at room temperature for 20 minutes followed by flow cytometry (Beckman Coulter, Cytoflex) to determine the fraction of dead cells. Each individual condition was repeated in technical triplicates.

In vitro phagocytosis assay

Anti-CD47 induced macrophage engulfment was evaluated using a phagocytosis assay (26). GFP-luciferase transfected 639V bladder cancer cells were removed from plates using 1x TrypLE (Gibco), washed with serum-free PBS and incubated either with PBS alone, or PBS with anti-CD47 (8 μg/mL) or anti-CD47-IR700 (8 μg/mL) for 1 hour on ice in the dark. After incubation, cells were divided into irradiated (8 J/cm^2) and non-irradiated groups, resulting in 6 different experimental conditions. Each condition was repeated in technical triplicates. 100,000 cells were seeded per well into a 96-well plate (Corning, Costar 3474 Ultra-Low Attachment) for use in phagocytosis assays.

In vitro phagocytosis assays were performed as previously described (26). Briefly, mouse macrophages were differentiated from bone marrow of NSG transgenic mice through incubation with M-CSF which differentiates macrophages to the M2 (inhibitory) phenotype typically found in tumor infiltrate (18, 27). Unfractionated bone marrow cells were cultured in IMDM+GlutaMax (Gibco) supplemented with 10% FBS, 100 U/mL penicillin and 100 μg/mL streptomycin, and 10 ng/mL murine M-CSF (Peprotech US). Macrophages were washed twice with HBSS (Gibco) then incubated with 1x TrypLE for approximately 20 minutes in humidified incubators at 37°C. Macrophages were removed from plates using cell lifters (Corning) then washed twice with serum-free IMDM and labeled with Alexa 647.

Phagocytosis reactions were carried out using 50,000 macrophages and 100,000 of the cancer cells treated as describe above, co-cultured for two hours at 37°C. After co-culture,

cells were washed with autoMACS Running Buffer (Miltenyi Biotec) and prepared for analysis by flow cytometry (BD Biosciences, LSRFortessa) equipped with a high-throughput sampler. Phagocytosis was evaluated as the percentage of Alexa647/GFP double positive macrophages using FlowJo v9.4.10 software (Tree Star) and was normalized to the maximal response. Phagocytosis assays were replicated three times in each individual condition.

In vitro NIR-PIT of patient-derived primary bladder cancers

With approval from Stanford Institutional Review Board and the VA Research and Development Committee, tumor tissue samples from patients (n=5) undergoing bladder cancer surgery (i.e. TURBT or radical cystectomy) at Stanford University Hospital and VA Palo Alto Health Care System were collected. Tumor grade and stage were determined by standard surgical pathology.

To obtain single cell suspension, tissue samples (~5 × 5 mm) were mechanically minced followed by a two-step digestion at 37°C using Collagenase IV (Worthington Biochemical) for 50 minutes and 1x TrypLE for 30 minutes. The cell suspension was washed with PBS and filtered through a 40 μm nylon strainer. The single cell suspension was then washed with PBS and incubated with PBS alone or anti-CD47-IR700 (8 μg/mL) for 1 hour on ice in the dark. Fifty thousand cells per well were seeded into 96-well low adhesion plates. For the NIR-PIT group, cells were first incubated with anti-CD47-IR700 followed by irradiation at 1, 2, 5, 10, 20 or 40 J/cm^2 as described above. In the anti-CD47-IR700 group, no irradiation was performed. After 30 minutes, propidium iodide was added to achieve final concentration of 1 μg/mL and incubated at room temperature for 20 minutes, followed by flow cytometry. Technical triplicates were performed for each experimental condition.

Human bladder cancer xenografts

Animal experiments were conducted in compliance with the Guide for the Care and Use of Laboratory Animal Resources (1996), US National Research Council, and approved by the local Animal Care and Use Committee. For all procedures, animals were anesthetized with isofluran (Fluriso).

Human bladder cancer xenografts were generated through engraftment of GFP-luciferase transfected 639V cells in immunocompromised NSG (Nod.Cg-Prkdc^{scid}Il2rgtm ^{1Wjl}/SzJ) mice (28). NSG mice lack B, T, and NK cells, but retain macrophages with phagocytic potential (18). Approximately 150,000 639V cells in 50% regular matrigel (Corning) were engrafted to the back of 6 to 10 week-old male NSG mice. For verification of engraftment and surveillance of tumor growth, mice were injected intraperitoneally with 200 μL D-Luciferin (16.66 mg/mL) after which bioluminescence was measured using IVIS Spectrum (PerkinElmer). Imaging was performed over 15-minutes to record maximal radiance. Region of interest (ROI) to measure peak total flux values were placed on the tumor and Living Image 4.5 (Caliper Life Sciences) was used for analysis. IVIS imaging frequency was mainly based on availability of the IVIS Spectrum and usually between 3-7 days. Mice were sacrificed after tumors reached either 20 mm diameter, a volume of 2000 mm^3 (calculated by the formula (length × width^2) × 0.5, or 30 days after the first experimental time-point.

In vivo NIR fluorescence imaging of anti-CD47-IR700 uptake in xenografts

For *in vivo* imaging, 200 μL of 1mg/mL anti-CD47-IR700 was administered via tail vein injection in tumor bearing mice. *In vivo* uptake of anti-CD47-IR700 in the mice was measured using the Pearl imager (LI-Cor Biosciences). For fluorescence intensity of the tumor in relation to the background, regions of interest (ROIs) were placed on the tumor and on adjacent background and a target-to-background ratio was calculated. In both the anti-CD47-IR700 and NIR-PIT groups, NIR fluorescence imaging was performed following anti-CD47-IR700 injection. In the anti-CD47-IR700 group (n=7), fluorescence imaging over 14 days was performed. In the NIR-PIT group (n=7), fluorescence imaging over 3 days was performed and irradiation doses of 100 and 50 J/cm^2 were performed after imaging on days 1 and 2, respectively.

In vivo NIR-PIT of human bladder cancer xenografts

The NIR-light was directed only at the tumor while the mouse was anaesthetized using the same LED setup as used in the *in vitro* experiments. For *in vivo* evaluation of single treatment of NIR-PIT, mice were divided into 4 groups: 1) control group (n=8) with no intervention; 2) anti-CD47-IR700 only group (n=7) with tail vein injection of 200 μg anti-CD47-IR700 and no irradiation; 3) irradiation only group (n=7) treated with 100 J/cm^2 on day 1 and 50 J/cm^2 on day 2); and 4) NIR-PIT group (n=7) was injected with 200 μg anti-CD47-IR700 (day 0) followed by irradiation regimen described for group 3.

To evaluate effects of repeated treatment of NIR-PIT in the xenograft model, a time course experiment was conducted consisted of 3 groups:1) control group (n=7) with no intervention; 2) anti-CD47 only group (n=7) with weekly tail vein injection of anti-CD47 for 5 weeks; and 3) NIR-PIT group (n=7) with irradiation at day 1 (100 J/cm^2) and day 2 (50 J/cm^2) after tail vein injection of 200 μg anti-CD47-IR700 at week 1 as above. For weeks 2 to 5, mice were treated with NIR-PIT (100 J/cm^2 at one day following anti-CD47-IR700 injection) weekly.

To examine the histopathological effects of NIR-PIT, a representative animal was sacrificed 24 hours after injection of anti-CD47-IR700 and tumor excised. The tumor was imaged on the Pearl imager (LI-Cor Biosciences) to confirm the co-localization of anti-CD47-IR700 and then frozen in optimal cutting temperature compound (OCT). After cyrosectioning of the tissue 10 μm sections were post-fixed in 4% paraformaldehyde for 30 minutes and imaged with a Zeiss LSM800 confocal microscope bright field imaging as well as NIR imaging at 700 nm.

Harvested tumors were fixed in 10% neutral buffered formalin for 24 hours, then embedded in paraffin blocks and sectioned at 5 μm. Immunohistochemistry was conducted using a primary antibody against the murine macrophage marker F4/80 (AbCam clone 8) with a dilution of 1:100. Microscopy images were obtained using a Leica DM5500B microscope.

Statistical analysis

Statistical analysis was carried out using statistical software Prism (GraphPad) and SAS. Descriptive statistics were expressed as mean ± standard error of the mean (SEM). For the *in*

vitro assays using bladder cancer cell lines and primary bladder cancer cells, unpaired t-test was used to assess differences in percent cell deaths between control and experimental groups. Two-way ANOVA was applied to determine the percent phagocytosis between control and experimental groups. For the *in vivo* xenograft experiments, $p<0.05$ was used as an indicator of statistical significance and one-way ANOVA with repeated measures with Tukey adjustment was used for multiple comparisons of fluorescence intensity. Survival analysis applying log-rank tests were used to determine the median survival time between control and the experimental groups, as displayed by Kaplan-Meier curves.

Results

In vitro NIR-PIT of CD47-expressing human bladder cancer cell lines

We first evaluated anti-CD47-IR700 mediated NIR-PIT in three human bladder cancer cell lines that express CD47: UMUC3, 639V, and HT1376 (Fig. 1 and Supplementary Fig. 1). Cultured cells were incubated with anti-CD47-IR700 then exposed to increasing doses (1 to 40 J/cm^2) of a 690-710 nm LED to induce NIR-PIT (Fig. 1). To measure direct cytotoxicity following NIR-PIT, flow cytometry using propidium iodide was used to assess the fraction of dead cells. Non-irradiated cells and unlabeled anti-CD47 were used as controls. In all three cell lines, NIR-PIT resulted in increased cell death in a light-dose-dependent manner. Significant cell death started at 2 J/cm^2 in 639V and HT-1376, and 5 J/cm^2 in UMUC3, and cell death rates increased with increased energy for all cell lines. At the maximum applied level of irradiation of 40 J/cm^2, over 90% of 639V and UMUC3 cells and over 50% of HT1376 died (Fig. 1A).

Anti-CD47 has been shown to promote phagocytosis of CD47 expressing cancer cells through blockage of the CD47-SIRPα interaction (18). Therefore, we investigated if anti-CD47-IR700 NIR-PIT could act to both induce cell death and promote phagocytosis. 639V cells were incubated with anti-CD47-IR700 followed by irradiation with 8 J/cm^2 of NIR light (Fig. 1B). 8 J/cm^2 was chosen based on the dose-escalation experiments (Fig. 1A), as it induced modest cytotoxicity and allowed for quantitation of the additive effects of NIR-PIT and anti-CD47-IR700 on phagocytosis. Phagocytosis of 639V was measured under six different conditions: incubation with PBS, anti-CD47 or anti-CD47-IR700, and with and without irradiation. After each experimental condition, cells were incubated with Alexa 647 positive mouse macrophages and the fraction of double positive (Alexa 647 and GFP) cells was determined by flow cytometry as an indicator of phagocytosis. Both anti-CD47 and anti-CD47-IR700 significantly induced phagocytosis compared to the no antibody controls. Without irradiation phagocytic activity was similar in the anti-CD47 and anti-CD47-IR700 groups. However, after irradiation phagocytic activity was significantly increased ($p=0.0002$) in the anti-CD47-IR700 group compared to the anti-CD47 group, which remained unchanged. This suggests that anti-CD47-IR700 can have dual functions of inducing direct cell death via NIR-PIT and enhancing phagocytosis (Fig. 1B).

In vitro NIR-PIT of primary human bladder cancer cells

To further assess the cytotoxic effects of anti-CD47-IR700 NIR-PIT, we tested primary bladder cancer cells derived from fresh tissue samples obtained during bladder cancer

surgery (Fig. 2). Bladder cancer specimen were harvested from five male patients during TURBT (n=4) or radical cystectomy (n=1). Single cell suspensions of approximately 50,000 primary bladder cancer cells were prepared and treated with NIR-PIT as described above. In the experimental group, primary cancer cells incubated with anti-CD47-IR700 were irradiated with increasing light doses from 1 to 40 J/cm^2. Non-irradiated cancer cells were used as control ("no light"). In all 5 primary human bladder cancer samples, cell death increased in a light-dose dependent manner (Fig. 2). Starting form light-doses of 5 J/cm^2 significant cancer cell death rates increased with increased energy to the maximum applied light dose of 40 J/cm^2, where over 75% of cancer cells died in 4 patient samples and over 55% cancer cells died in one patient sample. Pathological analysis was used to confirm the stage and grade of the tumor tissues with T2 high grade in two patients, Ta high grade in two patients and Ta low grade in one patient.

Evaluation of *in vivo* NIR fluorescence imaging of anti-CD47-IR700 uptake in xenografts

To assess the effects of anti-CD47-IR700 NIR-PIT in the context of a tumor we used a mouse xenograft model (Fig. 3). The GFP-luciferase transfected 639V cell line was chosen for engraftment into mice to facilitate visualization of tumors by luciferase bioluminescence. Anti-CD47-IR700 was administered via tail vein injection. First, we evaluated anti-CD47-IR700 localization and enrichment in the engrafted tumors. To visualize the anti-CD47-IR700 in the xenograft model over time, we performed IVIS and NIR fluorescence imaging in the tumor-bearing animals (n=7) over a course of 14 days after injection of antibody to colocalize tumor and antibody accumulation (Fig. 3A and 3B). Fluorescence intensity was enriched in the tumor starting one hour after injection, reaching a peak after 1 day and slowly decreasing thereafter (Fig. 3B and 3C). The tumor-to-background ratio increased over the first 10 days post-injection and plateaued thereafter up to day 14 (Fig. 3D). In all animals, the anti-CD47-IR700 fluorescence could be detected in the tumor for at least 14 days. Microscopic analysis at 24-hours post-infusion confirmed tumor penetration of anti-CD47-IR700 (Fig. 3E). Taken together, these results suggest killing of cancer cells at the site of accumulated antibody.

After observing in the 639V xenograft model that tumor NIR fluorescence intensity peaks at 24 hours after anti-CD47-IR700 injection, we treated the tumor with NIR-PIT at 24 and 48 hours and compared the NIR fluorescence intensity with the matching control (anti-CD47-IR700), which was injected but not irradiated. As seen in Figure 4 and further expanded below (Fig. 5), the tumor NIR fluorescence intensity was comparable in both groups before the treatment. After NIR-PIT, there was a sharp drop in tumor NIR fluorescence intensity in the tumors of the treated animals compared to non-irradiated controls.

Evaluation of *in vivo* therapeutic effect of CD47-targeted NIR-PIT in bladder cancer xenograft model.

To determine the therapeutic effects of CD47-targeted NIR-PIT we followed tumor growth in the 639V xenograft model after a single treatment of NIR-PIT (Fig. 5). The *in vivo* treatment irradiation dosing and timing was based on a previous report of *in vivo* EGFR-targeted NIR-PIT in bladder cancer xenograft model (11). For our experiment, tumor bearing mice were divided into control and treatment groups that included untreated mice,

irradiation only, antibody only without irradiation and CD47-targeted NIR-PIT. Following anti-CD47-IR700 injection, the mice were exposed to 100 J/cm^2 at 24 hours, then a second dose of 50 J/cm^2 at 48 hours. As measured by the tumor bioluminescence of the 639V cells, the mice in the NIR-PIT group showed significantly slower tumor growth than the mice in the no treatment and irradiation only groups ($p<0.0001$ and $p=0.0179$, respectively) (Fig. 5B). Tumor growth was modestly slower in the CD47-targeted NIR-PIT group than in the anti-CD47 alone group, however statistical significance was not reached (Fig. 5B).

To evaluate whether anti-CD47-IR700 NIR-PIT induced an influx of macrophages into the tumor we performed immunohistochemistry on tumor tissue samples from the xenograft models using the murine specific macrophage marker F4/80 (29). The small sample size precluded full statistical analysis, however, a trend towards higher macrophage numbers and a higher macrophage density within the tumors after injection of anti-CD47-IR700 was found in both the irradiated and non-irradiated mice compared to the control groups without anti-CD47-IR700 administration (Fig. 5D).

Analogous to standard clinical treatment protocols for localized bladder cancer (e.g. induction and maintenance intravesical therapy following TURBT), a potential clinical scenario for translation of CD47-targeted NIR-PIT would be intraoperative NIR-PIT directly after TURBT, then weekly NIR-PIT over a given time course. Therefore, we evaluated if repeated CD47-targeted NIR-PIT would yield more sustained reduction in tumor growth in the xenograft mice. In this experimental design (Fig. 6A) 639V xenograft mice were treated with anti-CD47-IR700 NIR-PIT as describe in Figure 5, then given weekly injections of anti-CD47-IR700 and a single direct dose of NIR-PIT at 100 J/cm^2 1-day post injection. A 5-week treatment regimen was implemented. Mice in the weekly CD47-targeted NIR-PIT group showed significantly less tumor growth compared to mice in the control group as well as in the repeated anti-CD47 only group ($p=0.0104$ and 0.0096 respectively) (Fig. 6B and 6C). Minor skin damage with signs of burn marks and small areas of necrotic skin tissue from repeat NIR dosing that healed between treatments was seen in 6 out of 7 animals. Importantly, the repeat NIR-PIT scheme kept tumors in check and resulted in significantly longer survival ($p=0.009$) compared to the control animals (Fig. 6D).

Discussion

Optimal detection, resection, and therapies for early stage bladder cancer are critical to prevent recurrence and progression of disease. CD47 is an innate immune checkpoint and a promising diagnostic and therapeutic target for bladder cancer. CD47 is highly expressed on the surface of bladder cancer cells but absent from the normal umbrella cells lining the bladder (18, 20, 21). Previously, we demonstrated molecular imaging of bladder cancer using topically administered, fluorescently-labeled anti-CD47 in intact human radical cystectomy specimens and found a diagnostic sensitivity of 82.9% and specificity of 90.5% for bladder cancer (21). Here we present the feasibility of molecular targeted PIT for bladder cancer using a CD47 antibody.

We found that CD47-targeted NIR-PIT induced cytotoxicity in a light-dose dependent manner in established CD47-expressing human bladder cancer cell lines and primary

bladder cancers cells from fresh surgical specimens, with up to 97.5% NIR-PIT specific cell death at the highest energy level tested. In xenograft models of human bladder cancer, a single treatment of NIR-PIT significantly decreased tumor growth compared to untreated animals and NIR light exposure alone. While tumors in the NIR-PIT treated animals trended smaller than tumors in the anti-CD47 alone group the difference did not reach statistical significance likely due to the relatively small number of animals and wide variation in tumor size. With weekly NIR-PIT treatment over a course of 5 weeks we found NIR-PIT with anti-CD47-IR700 resulted in significantly more durable tumor control and significantly longer survival compared to both untreated animals and anti-CD47 treatment alone.

Compared to conventional PDT, tumor targeting with a monoclonal antibody increases the specificity of NIR-PIT and decreases the potential for local side effects. Several molecular target/cancer combinations have been investigated for NIR-PIT, including PSMA for prostate cancer, PD-L1 for papillary adenocarcinoma of the lung, and EGFR for glioblastoma and bladder cancer, with similar light-dose dependent cancer cell killing for target expression cells *in vitro* and tumor control *in vivo* (15, 30, 31). Specifically, targeting EGFR to bladder cancer indicated that NIR-PIT selectively killed EGFR expressing bladder cancer cells *in vitro* (11). In line with our *in vivo* experiments applying a single round of NIR-PIT targeting CD47, in EGFR-based NIR-PIT attenuated tumor growth in xenografts of an EGFR expressing tumor cell line. However, no difference in tumor growth compared to controls was detected with NIR-PIT targeting EGFR in xenograft models with non-EGFR expressing bladder cancer cells (11). This demonstrates the importance of an abundantly expressed molecular target for broad therapeutic use. EGFR amplification is found in about 11% of bladder cancer (11, 16) therefore limiting the utility of EGFR targeted NIR-PIT for bladder cancer. A more abundant surface antigen, such as CD47, could lead to broader applicability of NIR-PIT in bladder cancer.

In addition to NIR-PIT, other strategies to develop targeted photosensitizer for urological cancer are under development. For example, Lin et al described a multifunctional nanoporphyrin platform using a bladder cancer-targeting peptide PLZ4 (32). They report promising results with the PLZ4-nanoporphyrin (PNP) in a patient-derived xenograft model of bladder cancer, showing PNP function integrating PDD, PDT, photothermal therapy (PTT) and targeted chemotherapy. While PNP as a theranostic approach has potential, it is still in its infancy and further trials are needed to evaluate its usefulness in bladder cancer. For localized prostate cancer, vascular-targeted photodynamic therapy using a water-soluble bacteriochlorophyll derived photosensitizer (WST11) is under clinical investigation. After systemic administration, the photosensitizer is activated to induced cell death by 753 nm NIR-light using optical fibers introduced via hollow needles in the prostate (33).

As a molecular target for bladder cancer therapy, CD47 has several advantages. Not only is it highly expressed on bladder tumors, blocking the CD47-SIPRα interaction with anti-CD47 promotes increased macrophage-mediated phagocytosis of CD47-expressing tumor cells (18). A distinguishing feature of our study is the combination of direct necrotic cell death from NIR-PIT and an increase in cancer cell phagocytosis mediated by the anti-CD47 antibody. The dual functions of anti-CD47-IR700 in NIR-PIT induced cytotoxicity and phagocytosis of tumor cells may enhance its therapeutic value, and potentially dose

reduction of NIR light. We demonstrated that IR700 conjugated anti-CD47 had similar function to promote cancer cell phagocytosis as the unlabeled antibody. To assay the additive effects of NIR, we exposed cells to an energy level of 8 J/cm^2 based on the finding that 5-10 J/cm^2 led to a moderate level of cell death. This provided an ideal scenario to assess combined NIR-PIT and macrophage-mediated phagocytosis, with cell kill by the initial dose of NIR irradiation, potentially injured cells and intact cells. The increased phagocytosis and cytotoxicity after NIR-PIT suggests that the dual function of anti-CD47-IR700 has an improved therapeutic value compared anti-CD47 alone. Consistent with its role in macrophage recruitment, immunohistochemistry of the tumor xenograft indicated an increased number and density of macrophages in the tumors treated with anti-CD47 and anti-CD47-IR700 (Fig. 5C).

Targeting CD47 with NIR-PIT may provide another additional biological therapeutic advantage. Calreticulin is a cell surface protein that confers an ‘eat me’ signal known to counterbalance the ‘don’t eat me’ signal conferred by CD47 (34). In line with previous reports showing some cytotoxic chemotherapies increase expression of calreticulin on tumor cells, Ogawa et al demonstrated that NIR-PIT also increased plasma membrane expression of calreticulin (35, 36). Therefore, increased pro-phagocytic calreticulin expression through NIR-PIT and blockade of the anti-phagocytic CD47 with anti-CD47 could provide additional tumor cytotoxicity.

While the results presented here are promising, this study has limitations. Our *in vivo* experiments rely on an established cell line in a xenograft model in NSG mice. Cell lines may not be representative of all bladder tumors, however the consistent response to NIR-PIT in the primary bladder cancer cells is indicative of the translation potential of our approach. Further, we utilized a xenograft model on the back of mice instead of orthotopic tumor growth directly in the bladder. We chose a non-orthotopic model because it offers more consistent tumor engraftment and enables superior monitoring of tumor growth, however the targeting and accumulation of antibody may vary in the different tumor models. Nevertheless, in combination with current clinical trials demonstrating the safety of both anti-CD47 therapy and NIR-PIT, we believe our results are strong enough to directly move towards clinical trials.

Repeat NIR-PIT may more efficiently kill tumor cells through increased permeability of the vasculature after the initial NIR-PIT thus facilitating antibody penetration ultimately leading to higher cytotoxicity rates (37). However, we noted photothermal skin damage with repeated NIR-PIT treatment, as others have reported with NIR-PIT (30, 38). Consequently, we modified our protocol and discontinued the second dose (50 J/cm^2 follow up dose at 24 hour) in the weekly repetition and irradiate the animal only with 100 J/cm^2 weekly. The skin lesions healed between NIR-PIT treatment in all but one animal. In future clinical applications in human bladders we believe that the impact of such a tissue damage is limited. Current standard of care transurethral resection of bladder tumors is performed by electrothermal cauterization that results in local tissue damage to tumor-adjacent normal tissue. Even after full thickness resection of the bladder wall into the perivesical fat the bladder typically heals with short term catheterization and appears normal at subsequent surveillance cystoscopy. Therefore, we envision that in future clinical application of NIR-

PIT as an adjunct to TURBT, additional photothermal tissue damage from NIR-PIT would not increase patient morbidity and recovery time from tumor resection. In addition, the light dose would need to be optimized to balance tumor control and minimize adverse effects.

Another future direction to pursue is the light source, as we used a LED light source instead of a laser, while others have reported an increased NIR-PIT induced cytotoxicity using a laser emitting 700 nm instead of a LED (39). Thus, a laser fiber energy source may improve the efficacy of anti-CD47-IR700 NIR-PIT and would also have the advantage that it easily could be inserted through a cystoscope for therapeutic translation.

The urinary tract is ideally suited for endoscopic targeted imaging and therapy due to ease of access. In addition to systemic administration of molecular therapeutic agents, topical administration offers an alternative/complementary route to enhance local concentration of the antibody. For bladder cancer insertion of a laser fiber through a cystoscope would allow for direct NIR dosing possibly resulting in fewer PIT side-effects when compared to external NIR-PIT. With a NIR cystoscopic camera, the fluorescence signal from IR700 would allow for intraoperative optical imaging thereby allowing the surgeon to improve tumor detection as well as assessment of resection margins to decrease recurrence rates. CD47-targeted NIR-PIT may be effective as a primary treatment for small multifocal tumor (e.g. in clinic setting) or disease with large surface area such as CIS. Additionally, NIR-PIT could be used as a supplement to TURBT to kill residual tumor cells after resection of the primary tumor. Molecular imaging in combination with targeted NIR-PIT may address the demands of specific imaging of the complete malignant lesion and precisely targeted treatment, thus offering an additional option in the armamentarium to treat bladder cancer. A weekly treatment protocol with NIR-PIT is also consistent with current practice of weekly treatment with intravesical BCG in patients with high risk NMIBC.

In summary, we show light dose dependent cytotoxicity of human bladder cancer cells with NIR-PIT using anti-CD47-IR700 as well as excellent *in vivo* tumor control. With additional clinical studies, we envision that anti-CD47-IR700 NIR-PIT could serve as adjuvant therapy after TURBT followed by weekly NIR-PIT treatment in an office-based setting to improve management of bladder cancer.

Supplementary Material

Refer to Web version on PubMed Central for supplementary material.

Acknowledgement:

BK was funded by Swiss National Foundation (P300PB 167793/1) and Bern Cancer League. JCL received funding support from NIH R01 CA160986 and Stanford University Department of Urology. ELR received funding support from NIH R01 CA190306. NSV was funded by the Netherlands Organization for Scientific Research (Rubicon, 019.171LW.022). We thank P.A. Beachy and A.M. Kershner for the helpful discussion, we thank S. Rogalla for help with IVIS imaging and we thank R.K. Mann for help with the interpretation of the mass spectrometry results. We thank D.R. Trivedi and T. Metzner for logistic support obtaining the primary bladder cancer specimen. We thank A. McCarty for breeding the NSG mice. We thank LI-COR for in kind gift of IRDye700DX.

References

1. Burger M, Catto JW, Dalbagni G, Grossman HB, Herr H, Karakiewicz P, et al. Epidemiology and risk factors of urothelial bladder cancer. Eur Urol. 2013;63(2):234–41. [PubMed: 22877502]
2. Sylvester RJ, van der Meijden AP, Oosterlinck W, Witjes JA, Bouffioux C, Denis L, et al. Predicting recurrence and progression in individual patients with stage Ta T1 bladder cancer using EORTC risk tables: a combined analysis of 2596 patients from seven EORTC trials. Eur Urol. 2006;49(3):466–5; discussion 75-7. [PubMed: 16442208]
3. Cambier S, Sylvester RJ, Collette L, Gontero P, Brausi MA, van Andel G, et al. EORTC Nomograms and Risk Groups for Predicting Recurrence, Progression, and Disease-specific and Overall Survival in Non-Muscle-invasive Stage Ta-T1 Urothelial Bladder Cancer Patients Treated with 1-3 Years of Maintenance Bacillus Calmette-Guerin. Eur Urol. 2016;69(1):60–9. [PubMed: 26210894]
4. van den Bosch S, Alfred Witjes J. Long-term cancer-specific survival in patients with high-risk, non-muscle-invasive bladder cancer and tumour progression: a systematic review. Eur Urol. 2011;60(3):493–500. [PubMed: 21664041]
5. Witjes JA. Bladder carcinoma in situ in 2003: state of the art. Eur Urol. 2004;45(2):142–6. [PubMed: 14733997]
6. Chang TC, Marcq G, Kiss B, Trivedi DR, Mach KE, Liao JC. Image-Guided Transurethral Resection of Bladder Tumors - Current Practice and Future Outlooks. Bladder Cancer. 2017;3(3):149–59. [PubMed: 28824942]
7. Burger M, Grossman HB, Droller M, Schmidbauer J, Hermann G, Dragoescu O, et al. Photodynamic diagnosis of non-muscle-invasive bladder cancer with hexaminolevulinate cystoscopy: a meta-analysis of detection and recurrence based on raw data. Eur Urol. 2013;64(5):846–54. [PubMed: 23602406]
8. Bader MJ, Stepp H, Beyer W, Pongratz T, Sroka R, Kriegmair M, et al. Photodynamic therapy of bladder cancer - a phase I study using hexaminolevulinate (HAL). Urol Oncol. 2013;31(7):1178–83. [PubMed: 22440147]
9. Lee JY, Diaz RR, Cho KS, Lim MS, Chung JS, Kim WT, et al. Efficacy and safety of photodynamic therapy for recurrent, high grade nonmuscle invasive bladder cancer refractory or intolerant to bacille Calmette-Guerin immunotherapy. J Urol. 2013;190(4):1192–9. [PubMed: 23648222]
10. Lee LS, Thong PS, Olivo M, Chin WW, Ramaswamy B, Kho KW, et al. Chlorin e6-polyvinylpyrrolidone mediated photodynamic therapy--A potential bladder sparing option for high risk non-muscle invasive bladder cancer. Photodiagnosis Photodyn Ther. 2010;7(4):213–20. [PubMed: 21112542]
11. Railkar R, Krane LS, Li QQ, Sanford T, Siddiqui MR, Haines D, et al. Epidermal Growth Factor Receptor (EGFR)-targeted Photoimmunotherapy (PIT) for the Treatment of EGFR-expressing Bladder Cancer. Mol Cancer Ther. 2017;16(10):2201–14. [PubMed: 28619755]
12. Shackley DC, Whitehurst C, Moore JV, George NJ, Betts CD, Clarke NW. Light penetration in bladder tissue: implications for the intravesical photodynamic therapy of bladder tumours. BJU Int. 2000;86(6):638–43. [PubMed: 11069369]
13. Mitsunaga M, Ogawa M, Kosaka N, Rosenblum LT, Choyke PL, Kobayashi H. Cancer cell-selective in vivo near infrared photoimmunotherapy targeting specific membrane molecules. Nat Med. 2011;17(12):1685–91. [PubMed: 22057348]
14. Dougherty TJ, Gomer CJ, Henderson BW, Jori G, Kessel D, Korbelik M, et al. Photodynamic therapy. J Natl Cancer Inst. 1998;90(12):889–905. [PubMed: 9637138]
15. Nagaya T, Nakamura Y, Sato K, Harada T, Choyke PL, Hodge JW, et al. Near infrared photoimmunotherapy with avelumab, an anti-programmed death-ligand 1 (PD-L1) antibody. Oncotarget. 2017;8(5):8807–17. [PubMed: 27716622]
16. Cancer Genome Atlas Research N. Comprehensive molecular characterization of urothelial bladder carcinoma. Nature. 2014;507(7492):315–22. [PubMed: 24476821]
17. Oldenborg PA, Zheleznyak A, Fang YF, Lagenaur CF, Gresham HD, Lindberg FP. Role of CD47 as a marker of self on red blood cells. Science. 2000;288(5473):2051–4. [PubMed: 10856220]

18. Willingham SB, Volkmer JP, Gentles AJ, Sahoo D, Dalerba P, Mitra SS, et al. The CD47-signal regulatory protein alpha (SIRPa) interaction is a therapeutic target for human solid tumors. Proc Natl Acad Sci U S A. 2012;109(17):6662–7. [PubMed: 22451913]
19. Oldenborg PA, Gresham HD, Lindberg FP. CD47-signal regulatory protein alpha (SIRPalpha) regulates Fcgamma and complement receptor-mediated phagocytosis. J Exp Med. 2001;193(7):855–62. [PubMed: 11283158]
20. Chan KS, Espinosa I, Chao M, Wong D, Ailles L, Diehn M, et al. Identification, molecular characterization, clinical prognosis, and therapeutic targeting of human bladder tumor-initiating cells. Proc Natl Acad Sci U S A. 2009;106(33):14016–21. [PubMed: 19666525]
21. Pan Y, Volkmer JP, Mach KE, Rouse RV, Liu JJ, Sahoo D, et al. Endoscopic molecular imaging of human bladder cancer using a CD47 antibody. Sci Transl Med. 2014;6(260):260ra148.
22. Advani R, Flinn I, Popplewell L, Forero A, Bartlett NL, Ghosh N, et al. CD47 Blockade by Hu5F9-G4 and Rituximab in Non-Hodgkin's Lymphoma. N Engl J Med. 2018;379(18):1711–21. [PubMed: 30380386]
23. Basa L Drug-to-antibody ratio (DAR) and drug load distribution by LC-ESI-MS. Methods Mol Biol. 2013;1045:285–93. [PubMed: 23913155]
24. Weiskopf K, Ring AM, Ho CC, Volkmer JP, Levin AM, Volkmer AK, et al. Engineered SIRPalpha variants as immunotherapeutic adjuvants to anticancer antibodies. Science. 2013;341(6141):88–91. [PubMed: 23722425]
25. Earl J, Rico D, Carrillo-de-Santa-Pau E, Rodriguez-Santiago B, Mendez-Pertuz M, Auer H, et al. The UBC-40 Urothelial Bladder Cancer cell line index: a genomic resource for functional studies. BMC Genomics. 2015;16:403. [PubMed: 25997541]
26. Majeti R, Chao MP, Alizadeh AA, Pang WW, Jaiswal S, Gibbs KD Jr., et al. CD47 is an adverse prognostic factor and therapeutic antibody target on human acute myeloid leukemia stem cells. Cell. 2009;138(2):286–99. [PubMed: 19632179]
27. Zhang M, Hutter G, Kahn SA, Azad TD, Gholamin S, Xu CY, et al. Anti-CD47 Treatment Stimulates Phagocytosis of Glioblastoma by M1 and M2 Polarized Macrophages and Promotes M1 Polarized Macrophages In Vivo. PLoS One. 2016;11(4):e0153550. [PubMed: 27092773]
28. Cheah MT, Chen JY, Sahoo D, Contreras-Trujillo H, Volkmer AK, Scheeren FA, et al. CD14-expressing cancer cells establish the inflammatory and proliferative tumor microenvironment in bladder cancer. Proc Natl Acad Sci U S A. 2015;112(15):4725–30. [PubMed: 25825750]
29. Austyn JM, Gordon S. F4/80, a monoclonal antibody directed specifically against the mouse macrophage. Eur J Immunol. 1981;11(10):805–15. [PubMed: 7308288]
30. Burley TA, Maczynska J, Shah A, Szopa W, Harrington KJ, Boult JKR, et al. Near-infrared photoimmunotherapy targeting EGFR-Shedding new light on glioblastoma treatment. Int J Cancer. 2018;142(11):2363–74. [PubMed: 29313975]
31. Nagaya T, Nakamura Y, Okuyama S, Ogata F, Maruoka Y, Choyke PL, et al. Near-Infrared Photoimmunotherapy Targeting Prostate Cancer with Prostate-Specific Membrane Antigen (PSMA) Antibody. Mol Cancer Res. 2017;15(9):1153–62. [PubMed: 28588059]
32. Lin TY, Li Y, Liu Q, Chen JL, Zhang H, Lac D, et al. Novel theranostic nanoporphyrins for photodynamic diagnosis and trimodal therapy for bladder cancer. Biomaterials. 2016;104:339–51. [PubMed: 27479049]
33. Azzouzi AR, Barret E, Bennet J, Moore C, Taneja S, Muir G, et al. TOOKAD(R) Soluble focal therapy: pooled analysis of three phase II studies assessing the minimally invasive ablation of localized prostate cancer. World J Urol. 2015;33(7):945–53. [PubMed: 25712310]
34. Chao MP, Jaiswal S, Weissman-Tsukamoto R, Alizadeh AA, Gentles AJ, Volkmer J, et al. Calreticulin is the dominant pro-phagocytic signal on multiple human cancers and is counterbalanced by CD47. Sci Transl Med. 2010;2(63):63ra94.
35. Obeid M, Tesniere A, Ghiringhelli F, Fimia GM, Apetoh L, Perfettini JL, et al. Calreticulin exposure dictates the immunogenicity of cancer cell death. Nat Med. 2007;13(1):54–61. [PubMed: 17187072]
36. Ogawa M, Tomita Y, Nakamura Y, Lee MJ, Lee S, Tomita S, et al. Immunogenic cancer cell death selectively induced by near infrared photoimmunotherapy initiates host tumor immunity. Oncotarget. 2017;8(6):10425–36. [PubMed: 28060726]

37. Ogata F, Nagaya T, Nakamura Y, Sato K, Okuyama S, Maruoka Y, et al. Near-infrared photoimmunotherapy: a comparison of light dosing schedules. Oncotarget. 2017;8(21):35069–75. [PubMed: 28456784]

38. Okuyama S, Nagaya T, Ogata F, Maruoka Y, Sato K, Nakamura Y, et al. Avoiding thermal injury during near-infrared photoimmunotherapy (NIR-PIT): the importance of NIR light power density. Oncotarget. 2017;8(68):113194–201. [PubMed: 29348898]

39. Sato K, Watanabe R, Hanaoka H, Nakajima T, Choyke PL, Kobayashi H. Comparative effectiveness of light emitting diodes (LEDs) and Lasers in near infrared photoimmunotherapy. Oncotarget. 2016;7(12):14324–35. [PubMed: 26885688]

40. Tseng D, Volkmer JP, Willingham SB, Contreras-Trujillo H, Fathman JW, Fernhoff NB, et al. Anti-CD47 antibody-mediated phagocytosis of cancer by macrophages primes an effective antitumor T-cell response. Proc Natl Acad Sci U S A. 2013;110(27):11103–8. [PubMed: 23690610]

Translational Relevance

Due to the high rate of recurrence and recognized shortcomings of standard endoscopic resection, new approaches to detection and treatment for localized bladder cancer are needed. NIR-PIT combines precise molecular targeting with light energy and is highly amenable in the urinary tract due to ease of access. CD47, a surface protein that blocks macrophage engulfment and an innate immune checkpoint, is highly expressed in bladder cancer but absent in normal luminal bladder cells thereby making CD47 a good therapeutic target. We report light dose-dependent CD47-targeted NIR-PIT induced cell death in human bladder cancer cell lines and primary human bladder cancer cells. In xenograft models of bladder cancer, anti-CD47-IR700 accumulated in tumors and NIR-PIT showed excellent tumor control with significantly reduced tumor growth rates and improved survival compared to untreated controls. CD47-targeted NIR-PIT can be deployed endoscopically and holds the potential to augment treatment of localized bladder cancer.

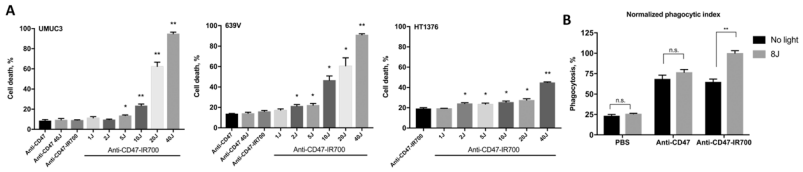

Figure 1. Anti-CD47-IR700 mediated photoimmunotherapy and phagocytosis of human bladder cancer cell lines.

A) CD47 expressing bladder cancer cell lines UMUC3, 639V and HT-1376 were incubated with 8 μg/mL anti-CD47-IR700 then irradiated with increasing doses from 1 to 40 J/cm^2 of NIR light or not irradiated. In 639V and UMUC3 cell lines were incubated with unlabeled anti-CD47 (8 μg/mL) without irradiation ("Anti-CD47") and with maximum irradiation dose ("Anti-CD47 40 J") to control for the effects of NIR irradiation alone. Direct cytotoxicity was measured by flow cytometry using propidium iodide for dead cell staining and counting. Bars represent technical triplicates for each condition. **B)** For the phagocytosis assay, 639V bladder cancer cells were first incubated with PBS, 8 μg/mL anti-CD47, or 8 μg/mL anti-CD47-IR700. After incubation cells were either irradiated (8J) or kept in the dark (No light) then combined with Alexa647$^-$labeled mouse macrophages. GFP-positive and GFP/Alexa647 double positive cells were counted by flow cytometry. Double-positive cells indicated macrophage engulfment of 639V cells. Without NIR-irradiation phagocytic activity was similar in the anti-CD47 and the anti-CD47-IR700 groups. After NIR-irradiation phagocytic activity was significantly ($p=0.0002$) increased in the anti-CD47-IR700 group compared to the unlabeled antibody. *$p < 0.05$, **$p<0.001$ comparison of treated groups vs. anti-CD47-IR700 (no light) control.

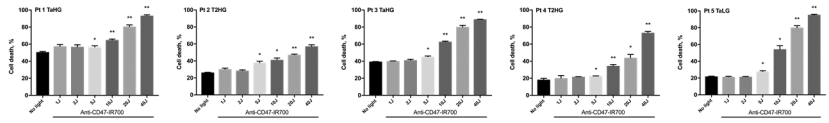

Figure 2. Anti-CD47-IR700 mediated photoimmunotherapy of primary human bladder cancer cells.

Fresh bladder tumor specimens of varying stage and grade from 5 different patients were digested to a single cell suspension of primary bladder cancer and incubated with 8 μg/mL anti-CD47-IR700 then irradiated with increasing doses of NIR-light from 1 to 40 J/cm^2. Non-irradiated cells were used as control (No light). Cytotoxicity induced by NIR-PIT was evaluated by flow cytometry using propidium iodide for dead cell staining and counting. *$p < 0.05$, **$p<0.001$ comparison of treated group vs. anti-CD47-IR700 (no light) control by student's t test. Abbreviations: Pt = patient; HG = high grade; LG = low grade

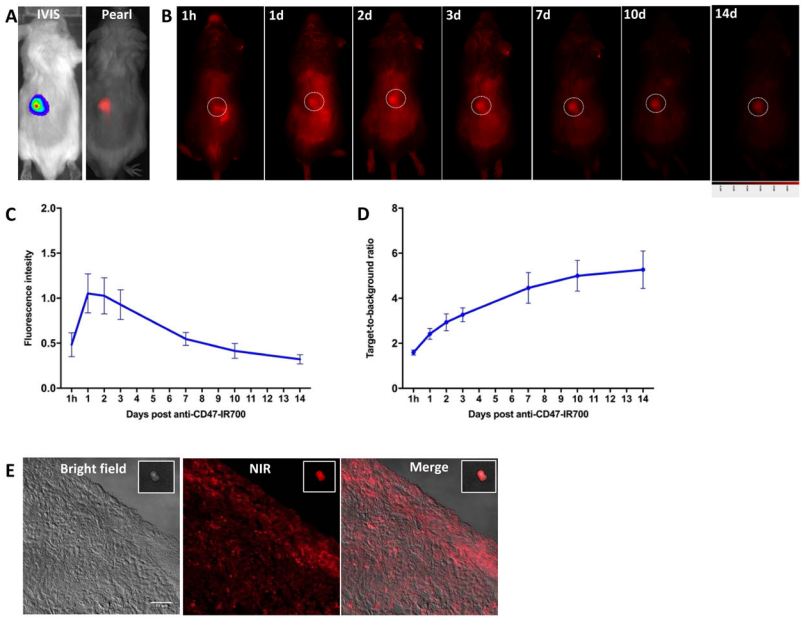

Figure 3. ***In vivo*** **near-infrared (IR700) fluorescence imaging and confocal microscopy of 639V xenograft tumors.**

After subcutaneous xenotransplantation of GFP-luciferase transfected 639V human bladder cancer cells to the back of male NSG mice, 200 μg anti-CD47-IR700 per mouse was administered via tail vein injection. *In vivo* IR700 fluorescence in tumor bearing mice (n=7) was visualized using a Pearl Imager (LI-Cor Biosciences) over a course of 14 days. **A)** IVIS for tumor bioluminescence and Pearl imaging for *in vivo* fluorescence showing colocalization of tumor and antibody. **B)** *In vivo* NIR fluorescence for representative animals at each time point. The tumor region, indicated by the white dotted circles, was determined by bioluminescence imaging. **C)** Quantitation of total IR700 fluorescence intensity at the tumor beginning one hour after anti-CD47-IR700 administration, then on a daily basis. **D)** Tumor-to-background ratio of the IR700 fluorescence. Regions of interests were placed on the tumor and background on adjacent non-tumor sites. **E)** In a representative animal, tumor was resected 24 hours after tail vein injection of anti-CD47-IR700. Confocal microscopy of the tumor using the 700-nm specific channel showed NIR fluorescence on the tumor surface as well as in the tumor-center indicating intratumoral penetration of the anti-CD47-IR700. The insets show bright field, near-infrared and merge images of the entire resected tumor.

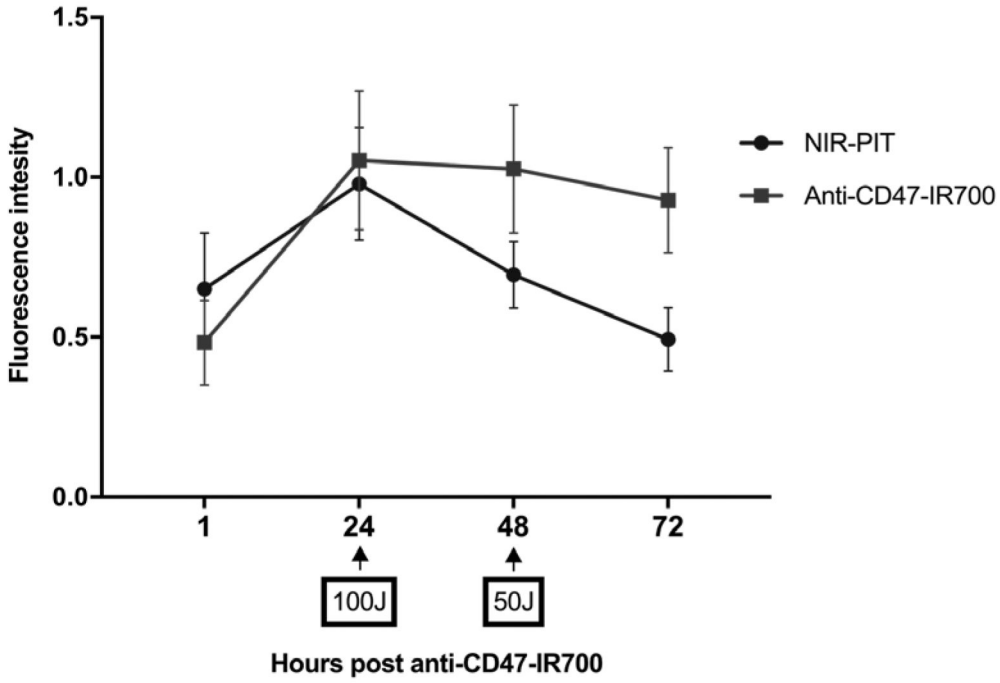

Figure 4. Comparison of *in vivo* IR700 fluorescence intensity of 639V tumors after NIR-PIT and control animals.

In vivo fluorescence imaging of animals 1, 24, 48 and 72 hours after tail vein injection of 200μg anti-CD47-IR700. The anti-CD47-IR700 only group (square marker, n=7) were not exposed to NIR light. The NIR-PIT animals (circular marker, n=7) received 100 J/cm^2 of NIR irradiation at 24 hours and 50 J/cm^2 at 48h after anti-CD47-IR700 administration. The NIR fluorescence intensity is notably decreased in the treatment group by 72 hours compared to the controls.

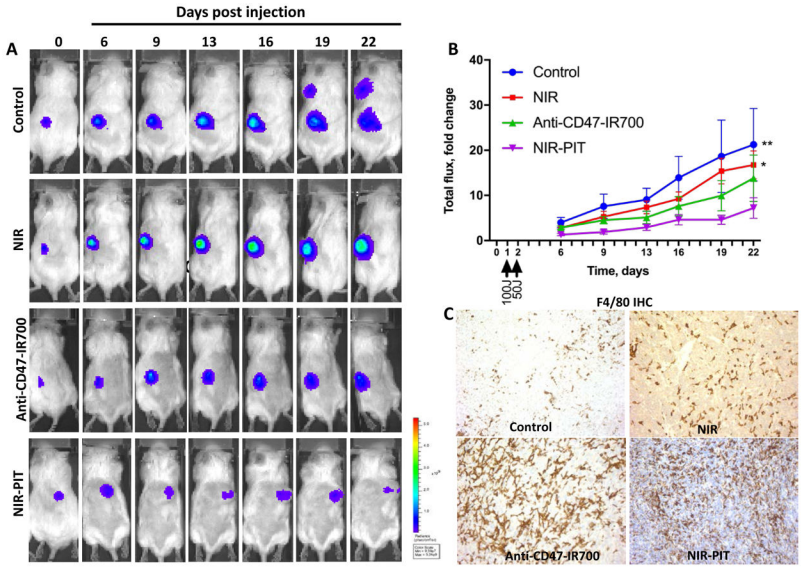

Figure 5. ***In vivo*** **tumor response to a single round of CD47-targeted NIR-PIT.**

Human bladder cancer 639V cells were transplanted subcutaneously to the back of male NSG mice and engraftment verified by bioluminescence. Tumor bearing mice were divided into 4 groups: 1) No treatment controls ("Control", n=8); 2) Irradiation only with no antibody injection ("NIR", n=7); 3) Anti-CD47-IR700 injection with no irradiation ("Anti-CD47-IR700", n=7); and 4) Anti-CD47-IR700 and irradiation ("NIR-PIT" n=7). NIR-irradiation was administered with 100 J/cm^2 at 24 hours after tail vein injection and a second dose of 50 J/cm^2 at 48 hours after tail vein injection. **A)** Bioluminescence images of representative animals over the time course showing tumor growth. Tumors in the NIR-PIT group were significantly smaller and more stable over the time period. **B)** Quantitative measurement of bioluminescence activity showing significantly larger tumor growth in the control group and NIR group respectively compared to the NIR-PIT group. *$p < 0.05$, **$p<0.001$ compared to the NIR-PIT group **C)** Immunohistochemistry of 639V tumors with the murine macrophage marker F4/80 show macrophage infiltration in all tumors. A trend towards higher macrophage numbers and density is noted in mice after anti-CD47-IR700 injection.

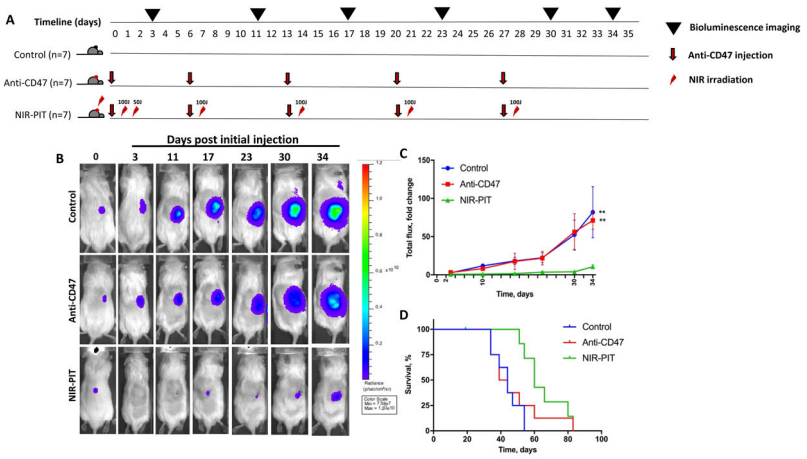

Figure 6. ***In vivo*** **tumor response to five rounds of CD47-targeted NIR-PIT.**

Xenograft tumors were generated in NSG mice as described for Figure 5. **A)** Experimental timeline indicates IVIS imaging to monitor tumor engraftment and treatment time points. After verification of 639V tumor cell engraftment animals were divided into 3 groups: 1) No treatment controls (n=7); 2) Anti-CD47 only (n=7); and 3) NIR-PIT receiving weekly tail vein injection of anti-CD47-IR700 followed by NIR-irradiation (n=7). **(B)** Bioluminescence images of representative animals over the time course showing tumor growth. Tumors in the repeated NIR-PIT group were stable over the period of NIR-PIT application and significantly smaller **(C)** Quantitative measurement of bioluminescence activity showing significantly larger tumor growth in the control and anti-CD47 only groups compared to the NIR-PIT group. Quantitative measurement of tumor volume is shown in Supplementary Figure 2. **(D)** Survival curve showing significantly longer survival in the NIR-PIT group (p=0.009).